A New Technique for Characterization of Early-age Cracking of Mortars

V. Lamour, A. Haouas & M. Moranville
LMT Cachan, Cachan, France.

R. Schell
RMC France, Rungis, France.

ABSTRACT: As the data for free shrinkage alone was found to be insufficient to predict the risk of early-age shrinkage cracking of restrained concrete, we developed a new technique to characterize the cracking phenomenon based on innovated ring-type specimen tests. The ring test consists of a concrete annulus that is cast around a hollow brass cylinder. As the mortar hydrates and dries, shrinkage is prevented by the ring resulting in the development of tensile stresses in concrete. With this experimental device, we were able to predict the risk of cracking in mortars. For this purpose two kinds of tests were defined: the semi-rigid ring, which allows a partial and constant restraint and the full-compensation system, using a pressurized cylinder around which the mortar was cast. Thus, we were able to follow the growth of internal properties of the material during aging such as, free shrinkage, restrained tensile stresses and visco-elastic response, which will provide precious information for future numerical implantation.

Keywords: cracking, mortar, free and restrained shrinkage, restrained ring-type specimens

1 INTRODUCTION

Most cementitious materials such as mortars undergo significant volume changes during both their construction phase (setting and hardening process) and their service life (desiccation, thermal and mechanical loading). For construction elements with a high surface/volume ratio like screeds, slabs and bridge decks, those volume changes are usually limited to autogeneous and drying shrinkage. The extent of shrinkage depends on the material properties, the external environment conditions such as temperature and moisture gradients and the degree of mechanical restraint. In many cases, when the tensile stress generated by the restraining support exceeds the strength of the screed that is quite low at the early-age, we have appearance of full-depth cracking. This can be damaging for the whole structure integrity since it becomes vulnerable to external attacks due to an increase of the permeability and a loss of mechanical resistance.

We present hereby our research investigations about the characterization tools we developed to test different formulations of mortar to be used in screed applications in restrained shrinkage conditions. These tools can also be generalized to many other applications such as aggregate concretes.

2 PROBLEMATIC

Shrinkage cracking of cementitious materials involves many different mechanisms that have to be combined to understand the global phenomenon of failure (shrinkage, friction of the support, stress generation, relaxation/creep, fracture behavior). For instance, free shrinkage measurements alone are not sufficient to characterize the cracking behavior of a screed glued to a rigid support, since a similar free shrinkage will cause cracks in a rigid, brittle material and no crack in a viscous, soft material. At a matter of fact, extensive knowledge of the mechanical behavior of the hardened material (strength, elastic behavior, creep function) is illusory as volumetric changes and hydration are strongly coupled to the mechanical properties in the very early ages. As a consequence, sophisticated experiments coupling continuous compensated shrinkage and visco-elastic properties measurements has been used to monitor the early age behavior of restrained sample under hydration and drying (Paillere et al. 1989, Tazawa 1998,

Pigeon et al. 2000, Altoubat & Lange 2001). However, during the setting phase, the experiments can not start until the highly viscous material has gained sufficient strength to be loaded. Secondly, the loading system becomes complicated as we want to compensate continuously the shrinkage of the sample.

3 EXPERIMENTAL

3.1 *Materials and mix proportions of mortars*

A large range of mortar formulations was tested in the experimental program but we will describe here only two kinds which represent a standard mortar showing early-age cracks (SM) versus an optimized one that resists to cracking (RM). We describe hereby the properties of the materials we used in those mortars

Table 1. Mortar compositions by weight of cement.

Material	Standard Mortar (SM)	Resisting Mortar (RM)
Cement	1	1
Special Sand Preparation	2.28	3.42
Fly Ashes	0	0.64
Superplasticizer: Polycarboxylatic ether type	0.011	0.018
Air Entraining Agent	0	0.026
Water/Binder weight ratio	0.5	0.54

Cement: The hydraulic cement used for both mortars was a Portland Cement CEM I 52.5 N CE CP2 NF (type I cement).
Fine aggregate: The aggregates used for the SM and the RM mortars were a well graded sand with a maximum diameter size of 4 mm.
Fly Ashes: a type C Fly Ash was used in the RM mortar with a 50% of SiO_2 , 29% of AL_2O_3 and 8.5% of Fe_2O_3 composition. (Use subscripts for the chemical compounds)
Superplasticizer: a polycarboxylatic ether type superplasticizer in addition to a diluted air entraining agent were used in RM mortar to increase the workability of the mortar (flow-screed mortar).
The compositions of the two mortars are presented in the Table 1.

3.2 *Description of the experiments*

The axi-symmetric geometry of an annular specimen cast on a rigid brass ring has been adopted for the simplicity of its restraining mechanism. Indeed with this experiment, shrinkage stress naturally develops without attaching any loading parts to the mortar or providing adequate end restraint. The feasibility of such a test has already been proved (Paillere et al. 1989, Swamy & Stavrides 1979, Grzybowski & Shah 1990, Weiss & Shah 2002 among others). The ring-type specimen tends to represent an infinite long and restrained pavement. However, one can show that the stress field in the mortar generated by the rigid ring slightly differs from the uniform longitudinal stress field we can obtain with a longitudinal restrained shrinkage test. In the first case, orthoradial traction stress field is non-uniform in the sample (the closer to the rigid ring, the greater is the orthoradial stress) and parasitic radial compression stress develops. The best lever to reduce those artifacts is the diameter of the ring as we can see on figure 1.

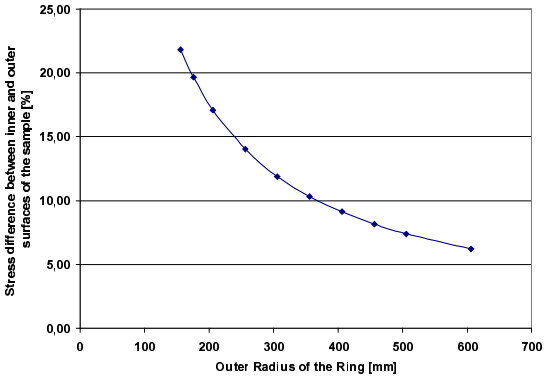

Figure 1. Scale effect on the heterogeneity of orthoradial stresses in the sample calculated by the finite element method (sample section 40x40 mm is kept constant)

Semi-rigid ring geometry

As a compromise between the uniformity of stresses and the volume of the sample, we chose an outer diameter of 300 mm for the semi-rigid ring and a sample section of 40x40 mm (giving 12% of difference between outer and inner orthoradial stress). The resulting friction between the mortar and the ring was minimized by choosing a brass ring so that orthoradial stress is constant around the sample. The choice of a 6 mm thickness for the brass ring is also the result of a compromise

between a sufficient rigidity of the restraining system and the sensitivity for the measurement of the deformation of the ring. Four orthoradial strain gages glued around the brass ring allowed the precise measurement of orthoradial strain and stress in the mortar sample (Figure 2).

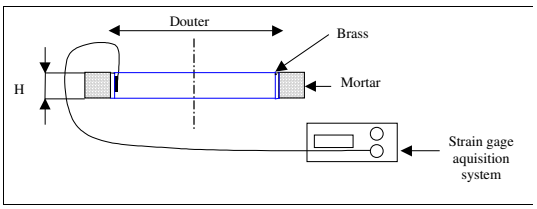

Figure 2. Schematic of the semi-rigid ring experiment

Shrinkage compensation system

In order to compensate completely the shrinkage and measure the stress field in the sample at the same time, we developed a new test based on a pressurized ring (figures 3 & 4).

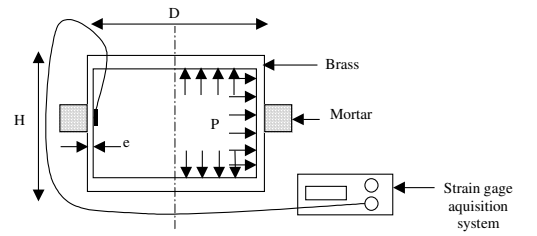

Figure 3. Schematic of the pressurized cylinder

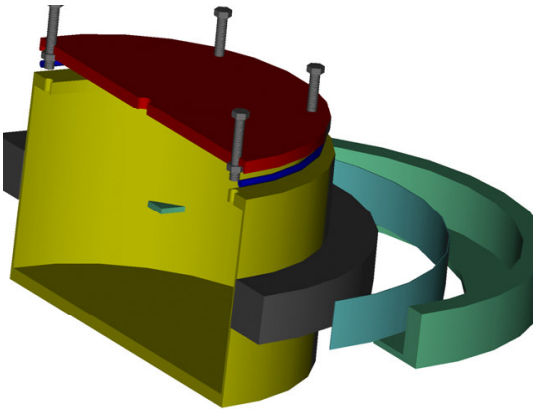

Figure 4. CAD view of the pressurized cylinder with mortar sample and mould

The sample geometry was kept constant for the same reasons as before (section 40x40 mm, inner diameter of 300 mm) whereas the brass cylinder was designed in order to obtain sufficient and uniform deformation in the mortar due to internal pressure (see figures 5 & 6 showing the Finite Element Method simulations).

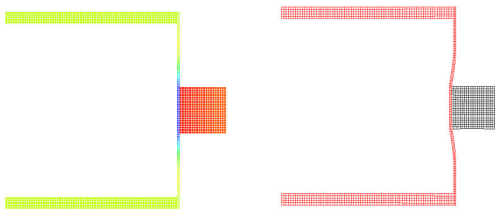

Figure 5. Field of orthoradial strain and deformation due to $200x10^{-6}$ free shrinkage enforced in mortar sample (elastic behavior of mortar with 15 GPa Young Modulus)

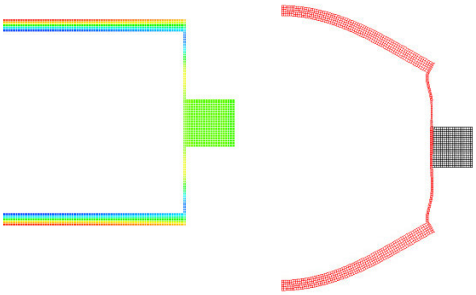

Figure 6. Field of orthoradial strain and deformation due to an internal pressure of 3 bars in the cylinder (elastic behavior of mortar with 15 GPa Young Modulus)

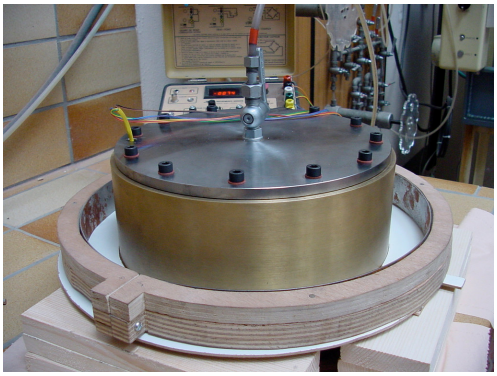

Figure 7. Views of the pressurized cylinder before casting the mortar

Four strain gages glued inside the tube were used to measure the deformation of the ring sample. The shrinkage restraint was then applied through a water pressure system inside the tube supplied by a Mercury column (limited to 4.5 bars). Figure 7 illustrates the experimental device before casting the mortar.

3.3 *Test procedures*

Strength tests

The compressive and flexural strengths of the mortars were measured on 40x40x160 mm prisms at the ages of 1, 3, 7, 10 and 28 days. The results showed that the resistant mortar (RM) had a reduced strength compared to the standard mortar (reduction of 47 and 21 percent respectively in compressive and flexural strength).

Free shrinkage tests

Two kinds of tests were carried out to measure the free shrinkage of the mortars. The first represented the free autogenous shrinkage on sealed samples and the second followed the total free shrinkage on specimens that were able to dry from all its faces. We should notice that these tests were performed in accordance with the ACTM C-341 (96) on 160-mm-long specimens with a 40x40-mm cross section. Figure 8 shows the results obtained from the second series. As expected, data of free shrinkage alone is not sufficient to predict the risk of cracking The difference of the total free drying shrinkage between the SM and the RM (24 %) is balanced by the difference in flexural strength (both mortars have similar Young's modulus).

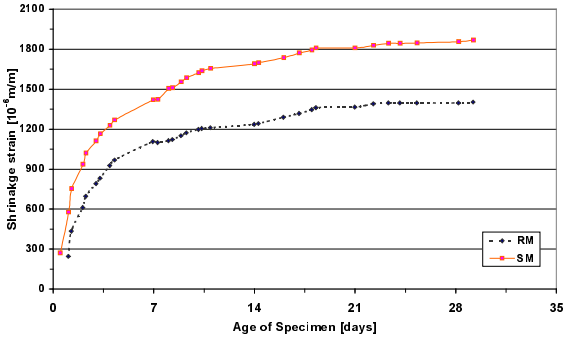

Figure 8. Free drying shrinkage strains measured for the standard mortar (solid line) and the resistant mortar (broken line)

Restrained shrinkage tests

The experiments carried out in this section concerned the semi-rigid and the elastic rings as they both represent restrained shrinkage systems but at two different degrees of restraint. The mortar was cast simultaneously around the two rings so that the data collected could be compared without any discordance.

Our first observation was the very early response obtained for both systems (Figure 9). Thus, we were able to follow the shrinkage-strain increase within the first 24 hours which corresponds to the formation of autogeneous shrinkage. The first compensation was applied after 14 hours which indicates the beginning of mortar hardening and the development of early shrinkage (Figure 10). The shrinkage was controlled by canceling manually the strains within a regular interval of time (each hour).

We should also notice that a pressure saturation may occur for these types of stiff mortars (see Figures 9 and 10 for the standard mortar SM) because the pressure is limited in the cylinder to 4.5 bars. For this reason, experiments on semi-rigid ring and on pressurized ring were conducted in parallel in order to obtain at the same time information about the development of restraining stress, the visco-elastic response of the material and the age of cracking.

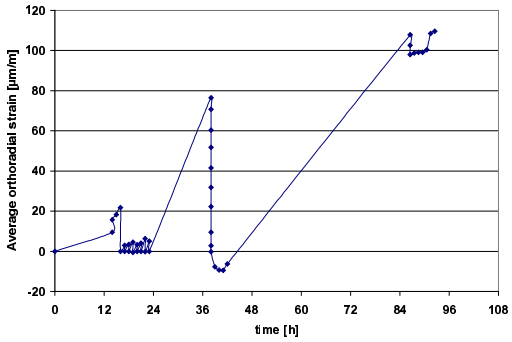

Figure 9. Shrinkage compensation procedure during setting and hardening of the standard mortar (SM)

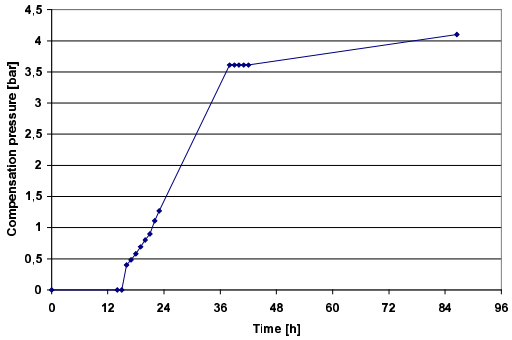

Figure 10. Evolution of compensation pressure in the brass cylinder for the standard mortar (SM)

4 PRELIMINARY RESULTS AND DISCUSSION

We present hereby a part of the experimental program we conducted on different formulations of mortars. As an example, cracking behaviors of the

standard mortar (SM) and a crack resistant mortar (RM) are compared through the ring techniques. Figure 11 represents the orthoradial stresses obtained from both mortars. The difference between the semi-rigid stress and compensated stress is expected as semi-rigid ring deforms slightly under the restraining stress.

After the saturation of the pressurized cylinder, semi-rigid stress data allow us to compare the behavior until failure of the partially restrained mortars. In this particular case, the crack resistant mortar exhibits a very low stress compared to the standard mortar after a few weeks of hydration and desiccation. Thus, after about 13.5 days from the beginning of the experiment, which corresponds to the age of cracking in the standard mortar, we reached the value of 4.1 MPa of tensile stress in the SM whereas we had just 1.7 MPa for the RM without any crack observed. The difference in the total orthoradial stress was then of 58 % between the two specimens tested.

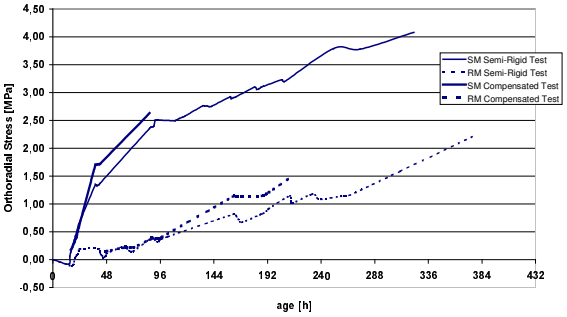

Figure 11. Generated orthoradial stress for semi-rigid (thin line) and compensated (thick line) shrinkage tests (dashed lines correspond to the crack resistant mortar)

This result can be explained by different free shrinkage but also by different visco-elastic properties. During the compensation procedure of the pressurized ring (Figure 9), we can approximately assess the apparent Young's modulus of the mortar between each step of pressure increase (visco-elastic response during an hour). The results are presented in Figure 12 showing indeed large differences between short term relaxation behavior and kinetics of stiffening (at the age of 7 days, the SM mortar developed an apparent Young's modulus of 27 GPa against 6 GPa for the RM mortar, which represents a decrease of approximately 79%).

A comparison between flexural strength of both mortars is also given in Figure 13. Although the standard mortar has a higher flexural strength (8.8 MPa against 5.2 MPa for the RM mortar), it develops larger shrinkage stress and cracks after a few weeks.

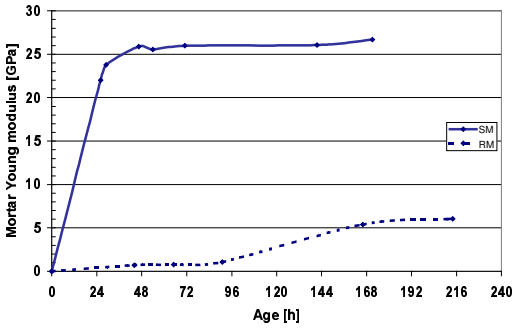

Figure 12. Mortar apparent Young's modulus extrapolated from the global rigidity of the pressurized cylinder during compensation (dashed line corresponds to the crack resistant mortar)

The large gap between flexural strength and tensile stress in Figure 13 (a decline of about 58 percent) results from the different loading speed and scale effects between the three-point bending and the compensated shrinkage tests (creep may occur in the second ones as a result of an imposed load that was maintained over the time).

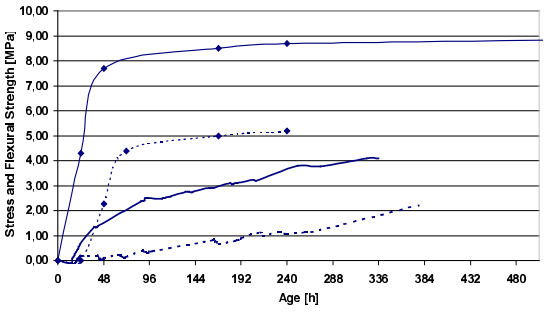

Figure 13. Comparison between orthoradial stress in semi-rigid ring sample and its flexural strength (dashed line corresponds to the crack resistant mortar)

From the fracture profile shown in Figure 14, we can check that the mortar failed due to tensile stresses.

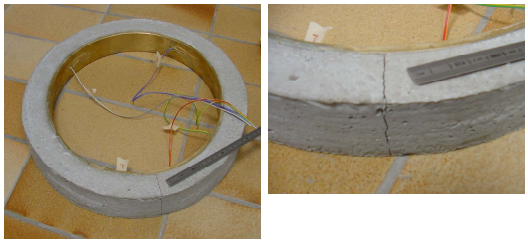

Figure 14. Views of the semi-rigid experiment after shrinkage cracking

5 CONCLUSION

A new technique based on ring tests has been proposed to monitor the shrinkage cracking resistance of mortars. The original aim of the tests was to reproduce the mechanical and hygro-thermal conditions during the construction and the service life of a screed, in order to validate different formulations in this application.

Two different mortars were presented in this study: a standard mortar that cracks easily and a low cracking potential mortar. The test set-up was composed of a semi-rigid ring, which allowed following the restrained material until failure and a total-compensated ring with which we were able to measure the development of the shrinkage stresses in fully restrained conditions.

We have shown that the designed tests gave a complete set of mechanical properties such as visco-elastic properties, tensile strength and crack resistance of the mortar, that allow a better understanding of its performance.

Further investigations are in progress with the perspective of developing the same tools for concretes with larger aggregates. In addition, thanks to continuous digital acquisition with several semi-rigid brass rings in parallel, we can study the effect of different hygro-thermal conditions on the cracking behavior of several materials.

6 REFERENCE

Paillere A.M., Buil M. & Serrano J.J. 1989. Effect of fiber addition on the autogeneous shrinkage of silica fume concrete, *ACI Materials Journal* 86, Mar-April 1989 : 139-144.

Tazawa E.I. (ed.) 1998. Autogeneous shrinkage of concrete. *Proceedings of the International workshop organized by Japan Concrete Institute*, E&FN Spon, London.

Pigeon M., Toma G., Delagrave A., Bissonnette B., Marchand J. & Prince J.P. 2000. Equipment for the analysis of the behavior of concrete under sustained shrinkage at early ages. *Magazine of Concrete Research* 52 : 297-302.

Altoubat S.A. & Lange D.A. 2001. Creep, shrinkage, an cracking of restrained concrete at early age, *ACI Materials Journal* 98, Technical Paper, July-August 2001 : 323-31.

Swamy R.N. & Stavrides H. 1979. Influence of fiber reinforcement on restrained shrinkage and cracking, *ACI Journal,* Technical Note, March 1979 : 443-52.

Grzybowski M. & Shah S.P. 1990. Shrinkage cracking of fiber-reinforced concrete, *ACI Materials Journal* 87, Mar-Apr 1990 : 138-148.

Weiss J. & Shah S.P. 2002. Restrained shrinkage cracking : the role of shrinkage reducing admixtures and specimen geometry, *RILEM Materials and Structures* 35, March 2002 : 85-91.

7 ACKNOWLEDGEMENTS

This work has been supported by RMC France. The authors would like to acknowledge Gérard Bernier for useful discussions about experiment design.